International Journal of Mechanical, Industrial and Aerospace Sciences
ISSN: 2517-9950
Vol:10, No:9, 2016

The Effect of Bottom Shape and Baffle Length on the Flow Field in Stirred Tanks in Turbulent and Transitional Flow

Jie Dong, Binjie Hu, Andrzej W Pacek, Xiaogang Yang, Nicholas J. Miles

***Abstract*—**The effect of the shape of the vessel bottom and the length of baffles on the velocity distributions in a turbulent and in a transitional flow has been simulated. The turbulent flow was simulated using standard *k-ε* model and simulation was verified using LES whereas transitional flow was simulated using only LES. It has been found that both the shape of tank bottom and the baffles' length has significant effect on the flow pattern and velocity distribution below the impeller. In the dished bottom tank with baffles reaching the edge of the dish, the large rotating volume of liquid was formed below the impeller. Liquid in this rotating region was not fully mixing. A dead zone was formed here. The size and the intensity of circulation within this zone calculated by *k-ε* model and LES were practically identical what reinforces the accuracy of the numerical simulations. Both types of simulations also show that employing full-length baffles can reduce the size of dead zone formed below the impeller. The LES was also used to simulate the velocity distribution below the impeller in transitional flow and it has been found that secondary circulation loops were formed near the tank bottom in all investigated geometries. However, in this case the length of baffles has smaller effect on the volume of rotating liquid than in the turbulent flow.

***Keywords*—**Baffles length, dished bottom, dead zone, flow field.

I. Introduction

STIRRED tanks are used in a wide range of processes such as solids dissolution, fermentation, gas absorption, extraction to name a few [1]. Despite the fact that in the industrial scale many of those processes are carried out in dished bottom vessels, majority of investigations of mixing in lab scale reported in literature were carried out in fully baffled flat bottom vessels [2]. Typically, the effect of the impeller type and speed on the overall flow pattern and energy dissipation rate distribution in a single phase [3]-[5] and in multiphase reactors [6], [7] were investigated. Detailed review of the modelling and simulation of flat bottom stirred tanks has been recently published [8], [9], therefore only the investigations of the stirred tanks fitted with Rushton turbine (used in this work) are briefly summarised below.

Bakker and Van den Akker [3] described characteristic turbulent flow pattern in fully baffled, flat bottom vessel agitated by Rushton turbine. The liquid jets from the turbine flow radially towards the tank wall, and upward and downward circulation loops are formed above and below the impeller. As the impeller was located at the clearance of one third of tank height, the downward circulation loop was smaller than the upward circulation loop. Bakker and Oshinowo [10] employed Large Eddy Simulation to model the large-scale chaotic structures generated by Rushton turbine in a flat bottom stirred tank. They found that the trailing vortexes formed behind each blade move towards the wall, which was also confirmed by the Large Eddy Simulation based on Lattice-Boltzmann method [11], [12].

Deglon and Meyer [13] investigated the effect of numerical methods and discretization schemes on the accuracy of simulations in a flat bottom stirred tank fitted with Rushton turbine. They showed that the Multiple Reference Frames (MRF) method and standard *k-ε* model accurately predict the trailing vortexes and enable accurate calculation of power number if very fine grid and higher-order discretization scheme are employed. But due to the deficiencies of standard *k-ε* model, the turbulent kinetic energy near the impeller region was still over or under-predicted. Aubin, Fletcher [14] have drawn the similar conclusions after they compared numerical simulation with Laser Doppler Velocimetry (LDV) measurements. They suggested that the discrepancies between predicted and measured turbulent kinetic energy near the impeller arise from the assumption of isotropy in *k-ε* model.

Deglon and Meyer [13] also compared the simulated flow profiles with LDV data of Wu and Patterson [15] and found that the experimental radial and tangential velocities near the impeller blades are deflected upwards whilst simulation showed that the velocity profiles near the impeller blades are symmetrical.

All studies mentioned above focused on the region around the impeller and flow pattern in the bulk and the flow region below the impeller were not discussed in their study.

In many industrial applications, especially in the processes carried out at elevated pressure condition, dished bottom stirred tanks are frequently used. But investigations of the flow pattern and energy dissipation rate distribution in such tanks are rather limited [16]. Deen, Solberg [17] reported that the shape of tank bottom had practically no significant effect on the flow pattern in the Rushton turbine region. However, this conclusion was based on the comparison of simulation results in a flat bottom tank with Particle Imaging Velocimetry (PIV) measurements in a dished bottom tank. The flow field outside impeller region

Binjie Hu is with the Department of Chemical and Environmental Engineering, The University of Nottingham Ningbo China, 199 Taikang East Road, Ningbo 315100, China (corresponding author: phone: +86(0)574 8818 0117, e-mail: Binjie.HU@nottingham.edu.cn).

Jie Dong, Xiaogang Yang and Nicholas J. Miles are with the Department of Chemical and Environmental Engineering, The University of Nottingham Ningbo China, 199 Taikang East Road, Ningbo 315100, China.

Andrzej W Pacek is with the School of Chemical Engineering, The University of Birmingham, Birmingham, Edgbaston, B15 2TT, UK.

was not discussed.

Aubin, Fletcher [14] simulated the flow field in a dished bottom vessel fitted with up and down pumping pitched blade turbines. They observed that in the dished bottom vessel the circulation loop is closer to the wall and has larger vorticity than the circulation loop in a flat bottom tank agitated by similar impeller [18]. They also concluded that numerical scheme is more important in predicting turbulent kinetic energy in a dish bottom vessel than in a flat bottom vessel. However, there is very small difference between their results obtained with standard k-ε and with Re-Normalization Group (RNG) k-ε model. The latter conclusion contradicts the results obtained in a flat bottom vessel where the prediction of turbulent kinetic with standard k-ε model was more accurate than prediction with other Reynolds averaged equations [19].

Ochieng and Onyango [20] reviewed the modelling of solids suspension in stirred tanks and concluded that dished bottom tanks fitted with Rushton turbine or pitched blade impeller are better suited for particle suspension than the flat bottom tanks, because in the former ones the dead zones at the wall junctions do not form. This is particularly important in the tanks with large aspect ratio.

The effect of the width and length of baffles on mixing process was investigated by several researchers. Lu et al. [21] found that the baffles greatly improve the liquid mixing even with very small ratio of baffle width to tank diameter ($B/T < 0.05$). The mixing time decreases sharply with the increase of baffles' width, and becomes constant when $B/T>0.1$. Karcz and Major [22] reported that the Rushton turbine power number decreases as the length of the baffles decreases in a turbulent flow in a flat bottom vessel. But the effect of baffles on the dead zones, mixing efficiency and flow pattern was not discussed. Haque et al. [23] simulated turbulent flow in an un-baffled dished bottom stirred vessel fitted with Rushton turbine and found that a vortex below the impeller was formed. Such vortex was not observed in a fully baffled flat bottom stirred vessel. They also concluded that standard k–ε model, shear-stress transport model and Reynolds-stress turbulence model give very similar results.

Compared with turbulent flow studies, numerical and experimental investigations on transitional flow in stirred tanks are limited. Jaworski et al. [24] simulated the transitional flow of shear thinning liquid in a fully baffled flat bottom stirred tank agitated by a Rushton turbine using sliding mesh method and RNG k–ε model. A good agreement was found between calculated and measured (using LDA) mean axial, radial and tangential velocities. Yang et al. [25] employed Detached Eddy Simulation and Volume of Fluid model to simulate the mixing time and mixing processes of initially stratified miscible fluids in a flat bottom stirred tank. The flow is agitated in transitional status. They found that the mixing time was slightly reduced by eccentric agitation at higher impeller speed. But the situation was reversed at low impeller rotation speed. Besides, the mixing uniformity cannot be improved by eccentric agitation of low viscosity miscible fluids starting from stratified state. Woziwodzki et al. [26] studied the effect of eccentricity on transitional mixing in unbaffled flat bottom stirred tank when multiple impellers were used. The role of shaft eccentricity and impeller combinations on power consumption and mixing time were investigated. They found that the two Rushton turbines impeller combination needs the shortest mixing time in all centrically located impeller combinations. The mixing time is decreasing as the eccentricity ratio from 0 to 0.42. When this ratio is larger than 0.42 the mixing time will start to increase.

This brief literature review clearly indicates that majority of theoretical and experimental studies of different aspect of mixing as well as the investigations of the accuracy of numerical models were conducted in a turbulent, fully baffled, flat bottom stirred vessel. As already mentioned in many industrial applications, pressurised dished bottom stirred reactors with baffles extending only to the dish level are used, but the effect of length of baffles and the shape of tank bottom on the flow field are not discussed in open literature. Also the information on the mixing of highly viscous fluids, such as ionic liquids, in a transitional flow is rather limited in open literature. To fill this gap, systematic numerical and experimental investigation of mixing in dished bottom vessels were undertaken. In this paper, the effect of bottom shape and the baffles' length on mixing in stirred tanks fitted with Rushton turbine has been investigated numerically.

II. Geometry of Stirred Tanks

The details and dimensions of stirred tanks used in this work are summarised in Fig. 1. The stirred tank is with tank diameter (T) and height (H) equals to 150 mm. The impeller-bottom clearance (C) is 75 mm. The impeller diameter (D) is 75 mm, with blade height w=15 mm and blade width b=18.75 mm. Fig. 1 (a) shows fully baffled flat bottom tank (FB tank) and Fig. 1 (b) shows dished bottom tank with baffles reaching dish level (DBD tank). Dotted lines in Fig. 1 (b) show the baffles extending to the tank bottom (DBB tank).

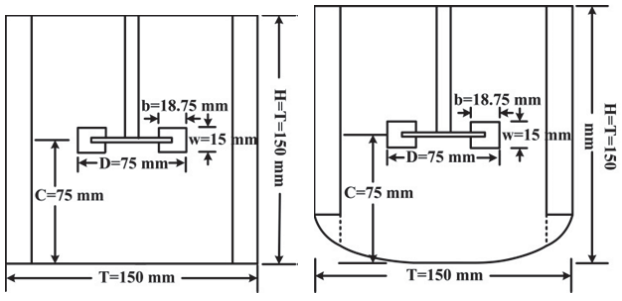

Fig. 1 Stirred tanks used in this work: (a) FB tank, (b) DBD tank and DBB tank (dotted lines)

The stirred tank used in experimental study is made from optical glass. The simulation was carried out with water ρ=998 kg/m^3, μ=0.001 Pa.s) and with ionic liquid ($BmimBF_4$, ρ=1210 kg/m^3, μ=0.07 Pa.s). The impeller speeds of 150 rpm for water (Re=14000) and 440 rpm for ionic liquid (Re=650) were determined experimentally to avoid bubbles entrainment during PIV measurement of velocity distributions.

III. Numerical Modelling

The ANSYS FLUENT (Version 14.5) was employed to simulate the flow by solving continuity [27]:

$$\frac{\partial(\rho\overline{u_i})}{\partial x_i} = 0 \tag{1}$$

and momentum balance:

$$\frac{\partial(\rho\overline{u_i}\,\overline{u_j})}{\partial x_j} = -\frac{\partial p}{\partial x_i} - \rho\overline{\overrightarrow{u_i'u_j'}} + \rho\vec{f} \tag{2}$$

equations for the incompressible, steady state turbulent flow in the stirred tanks. where ρ is the fluid density, $\vec{u}$ is the flow velocity vector, p is the static pressure, $\rho\vec{f}$ represents the body forces including gravity and buoyancy The turbulent stress, $\rho\overline{\overrightarrow{u_i'u_j'}}$, and the turbulent viscosity, μ_t, are calculated from:

$$-\rho\overline{\overrightarrow{u_i'u_j'}} = \mu_t\left(\frac{\partial\overline{u_i}}{\partial x_j} + \frac{\partial\overline{u_j}}{\partial x_i}\right) - \frac{2}{3}\rho k\delta_{ij} \tag{3}$$

$$\mu_t = \rho C_u\frac{k^2}{\varepsilon} \tag{4}$$

where C_μ is model constant equals to 0.09 in standard k-ε turbulence model, δ_{ij} is Kronecker delta (δ_{ij}=1 if i=j and δ_{ij}=0 if i≠j). k and ε are turbulent kinetic energy and turbulent kinetic energy dissipation rate calculated from [28]:

$$\frac{\partial}{\partial x_i}(\rho k\vec{u}_i) = \frac{\partial}{\partial x_j}\left[\left(\mu + \frac{\mu_t}{\sigma_k}\right)\frac{\partial k}{\partial x_j}\right] + G_k - \rho\varepsilon \tag{5}$$

$$\frac{\partial}{\partial x_i}(\rho\varepsilon\vec{u}_i) = \frac{\partial}{\partial x_j}\left[\left(\mu + \frac{\mu_t}{\sigma_\varepsilon}\right)\frac{\partial\varepsilon}{\partial x_j}\right] + C_{\varepsilon1}\frac{\varepsilon}{k}G_k - C_{\varepsilon2}\rho\frac{\varepsilon^2}{k} \tag{6}$$

$$G_k = -\rho\overline{u_i'u_j'}\frac{\partial\vec{u}_j}{\partial x_i} \tag{7}$$

where G_k represents the generation of k result from mean velocity gradients. Semi empirical constants: $C_{\varepsilon1} = 1.44$, $C_{\varepsilon2} = 1.92$, $\sigma_\varepsilon = 1.0$, $\sigma_k = 1.3$.

It was expected that the change of the bottom shape and the length of baffles might lead to the changes of the structure, size and position of the large scale energy containing eddies, therefore Large Eddy Simulation (LES) was also carried as it was reported that it is more accurate than the standard k-ε model and that is particularly useful if the large structures in the flow are of interest [29].

LES governing equations are obtained by spatial filtering out turbulent eddies smaller than the filter width and filtered continuity and momentum equations for incompressible flow take the form [27]:

$$\frac{\partial\rho}{\partial t} + \frac{\partial(\rho\overline{u}_i)}{\partial x_i} = 0 \tag{8}$$

$$\frac{\partial(\rho\overline{u}_i)}{\partial t} + \frac{\partial}{\partial x_j}\left(\rho\overline{u}_i\overline{u}_j\right) = -\frac{\partial\bar{p}}{\partial x_i} + \frac{\partial\tau_{ij}}{\partial x_j} + \frac{\partial\sigma_{ij}}{\partial x_j} \tag{9}$$

Subgrid scale Reynolds stress (σ_{ij}) is proportional to the local strain rate of the resolved flow:

$$\sigma_{ij} - \frac{1}{3}\sigma_{kk}\delta_{ij} = -2\mu_t\bar{S}_{ij} \tag{10}$$

where $\bar{s}_{ij}$ is the rate of strain tensor for the resolved scale:

$$\bar{s}_{ij} = \frac{1}{2}\left(\frac{\partial\overline{u}_i}{\partial x_j} + \frac{\partial\overline{u}_j}{\partial x_i}\right) \tag{11}$$

Smagorinsky-Lilly subgrid scale model was employed here which is widely used in modelling the effect of the unsolved small eddies on resolved large eddies in stirred vessels [30-32]. The turbulent viscosity μ_t and mixing length L_s are calculated from [28]:

$$\mu_t = \rho L_s^2|\bar{s}| \tag{12}$$

$$L_s = min(\kappa d, C_s V^{\frac{1}{3}}) \tag{13}$$

$$|\bar{s}| = \sqrt{2\bar{s}_{ij}\bar{s}_{ij}} \tag{14}$$

where κ is von Kármán constant equals 0.41, d is the distance from node to the closest wall. C_s is Smagorinsky constant equals 0. 1. V is cell volume.

MRF method was used to model the rotating impeller in steady-state turbulent flow field, and the Sliding Mesh method was employed in transient LES. In both methods the computational domain is divided into two zones: the rotating zone and the stationary zone. The rotating zone includes the impeller and a small part of impeller shaft, whereas stationary zone includes the domain outside rotating zone as shown in Fig. 2. A time step of 0.003 s was used to simulate water turbulent flow and 0.001 s was used to simulate ionic liquid transitional flow in LES.

The ANSYS ICEM CFD (Version 14.5) was used to mesh the geometry of stirred tanks. The structured hexahedral mesh that enables simple data handling and speeds up the calculations was employed [33].

Fig. 2 shows the geometry of stirred tanks after meshing. The effect of mesh size on the accuracy was investigated. The simulation was started from the coarse mesh with 660K, 650K, and 650K of nodes for FB tank, DBD tank and DBB tank respectively. The velocity profiles below the impeller were monitored at each mesh size. Nodes number of 920k, 860k and 880k were used for the FB tank, DBD tank and DBB tank respectively, the further increase of number of nodes did not affect velocity distributions.

For LES simulation, the meshes of three stirred tanks were further refined and the maximum grid size was reduced less than 2 mm. Around 1.60 million, 1.62 million and 1.65 million nodes were used for DBD, DBB and FB tanks respectively.

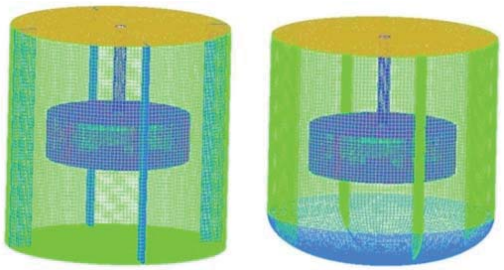

(a) (b)

Fig. 2 Mesh of stirred tanks: (a) FB tank, (b) DBB tank

IV. Results and Discussion

A. Effect of Bottom Shape and Baffles Length on Water Turbulent Flow Field

The time-averaged flow fields predicted by standard k-ε model in all three vessels are shown in Figs. 3 and 4. The velocity vectors in vertical symmetry planes between two adjacent baffles are shown in Fig. 3 which indicates that the flow is axially symmetrical with the circulation loops of similar intensity below and above the impeller.

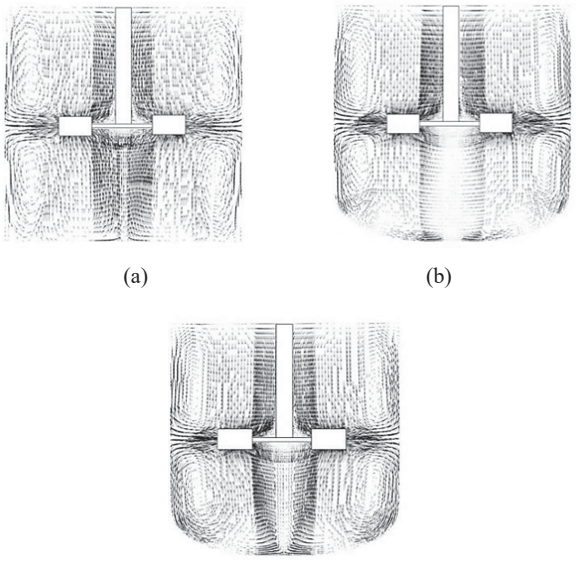

(a) (b)

(c)

Fig. 3 Velocity vectors in the symmetry planes between adjacent baffles: (a) FB tank; (b) DBD tank; (c) DBB tank

Whilst the velocity profiles in and above the impeller region are nearly the same in all geometries, the dish shape and length of the baffles greatly affect the velocity distributions in the region below the impeller as well as the region close to the tank bottom. The most significant difference among the three geometries is the conical/cylindrical and near stagnant volume just below the impeller in Fig. 3 (b) (DBD tank).

The visual detail of the flow vectors and contours below the impeller in different tanks are shown in Fig. 4. In the fully baffled flat bottom vessel (Fig. 4 (a)), stagnation zones exist at the bottom as well as near the corners between the bottom plane and cylindrical walls whilst there is a very intensive axial flow directly below the impeller. In dished bottom vessel with baffles reaching the edge of the dish (Fig. 4 (b)) the stagnation zones at the bottom practically disappeared.

A very large dead zone is formed below the impeller in DBD tank (Fig. 4 (b)). The diameter of this dead zone is almost one fifth of impeller diameter and it extends from the impeller to the bottom of the vessel. It has to be stressed here such a large dead zone in dished bottom vessels has not reported in numerical and experimental studies on flow hydrodynamics in stirred tanks. The presence of such a large dead zone not only has a negative effect on mixing in single phase systems, which might lead to an extensive coalescence in gas/ liquid systems, but also causes problems with suspending solid particles in liquid. The minimum impeller speed N_{JS} [1] which is necessary to suspend the particles is calculated from the empirical correlations based on experimental data obtained in a fully baffled flat bottom tanks. The above results clearly question applicability of such correlations to dish bottom tanks.

The size of the dead zone can be reduced by extending the baffles to the very bottom of the vessel as shown in Fig. 4 (c), which results in larger circulation loops and increase of velocity magnitude between the impeller and tank bottom (compare with Figs. 4 (b) and (c)). This reduces mixing time in single phase systems, prevents coalescence in gas/ liquid and liquid/ liquid systems and might also lead to the increase of minimum velocity of suspension in solid/ liquid systems.

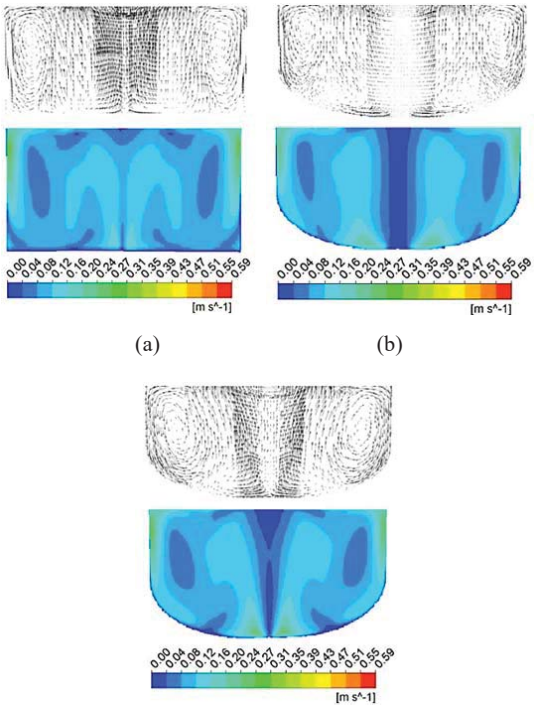

(a) (b)

(c)

Fig. 4 Velocity vectors and contours below the impeller in: (a) FB tank; (b) DBD tank; (c) DBB tank

The radial distributions of all velocity components in the horizontal plane (40 mm above the tank bottom) approximately half way between the bottom of the tank and the impeller in steady state simulations are calculated from below equations and shown in Fig. 5.

$$U_{radial}(r) = \frac{1}{2\pi}\int_0^{2\pi} U_{radial}(r,\theta)d\theta \quad (15)$$

$$U_{axial}(r) = \frac{1}{2\pi}\int_0^{2\pi} U_{axial}(r,\theta)d\theta \quad (16)$$

$$U_{tangential}(r) = \frac{1}{2\pi}\int_0^{2\pi} U_{tangential}(r,\theta)d\theta \quad (17)$$

where U_{radial} U_{axial} $U_{tangential}$ are mean radial, axial and tangential velocities respectively. r is the radial distance from plane centre to tank wall. The magnitude of velocity components were normalized by the impeller tip velocity U_{tip} (0.59 m/s). The radial distance (r) was normalized by tank radius R.

The simulation result shows that the shape of the tank bottom and the length of the baffles have virtually no effect on the radial velocity (Fig. 5 (a)) which is practically zero because the flow is mainly axial/ tangential in the cross section at half way between impeller and the tank bottom.

In contrast, the tangential and axial velocities in the region around the symmetry axis below the impeller are greatly affected by the bottom shape and baffle length. The axial velocities in the centre of this plane are drastic reduced from $0.2U_{tip}$ in FB tank to $0.06U_{tip}$ *in* DBB tank and to almost 0 in DBD tank followed by the gradual increase to the maximum at r=0.41R *in* DBD tank and to r=0.28R in DBB tank (Fig. 5 (b)). Nearly 40% of the volume below the impeller in DBD tank is poorly mixed in axial direction.

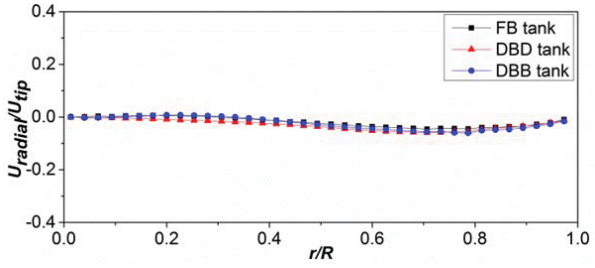

(a)

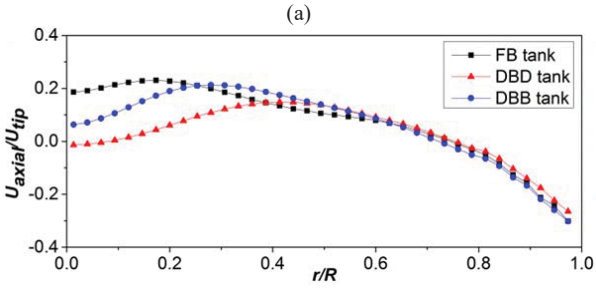

(b)

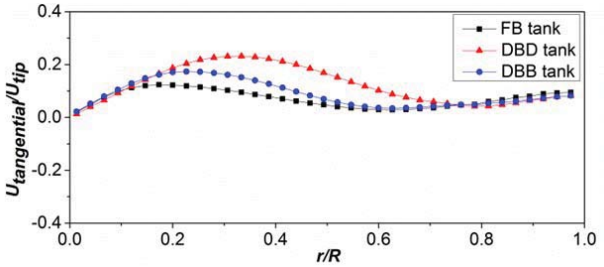

(c)

Fig. 5 Radial distributions of velocity components: (a) radial velocity; (b) axial velocity; (c) tangential velocity

The tangential velocity as shown in Fig. 5 (c) is even more sensitive to the bottom shape and baffle length. In the dished bottom tank fitted with shorter baffles (DBD tank), a forced vortex is formed below impeller. Around 35% volume of the liquid in the vortex region is rotating in tangential direction without efficient mixing.

Fig. 5 clearly indicates that reduction of velocity magnitude below the impeller is mainly caused by the reduction of axial velocity in this region. It is well known that the baffles prevent swirling and vortexing [21] and the relative velocities between the impeller and liquid are small without baffles which results in reduction of downwards pumping and in poor axial mixing [34] as observed in DBD tank. Mixing was drastically improved when baffles reached the tank bottom breaking the rotation of the liquid and increasing axial flow rate Lamarque, Zoppé [35]. In DBD tank, vortex was formed below the impeller with low tangential velocity at the vortex centre and high tangential velocity at edge. Similar inner vortex below the impeller in unbaffled dished bottom stirred tank agitated by Rushton turbine was mentioned by Haque, Mahmud [23]. The extending baffles to the tank bottom (the DBB and FB tank) can reduce the magnitude of the forced vortex and intensity of rotation liquid below the impeller, hence increase mixing efficiency in this area.

B. Large Eddy Simulation

As discussed above, one of the differences between investigated geometries is the magnitude and extension of forced vortexes formed below the impeller. The LES is better suited to simulation of large dynamic structures. The standard k-ε model is widely used to model the flow in fully developed turbulent state. The LES can reinforce the results predicted by standard k-ε model especially the existence of dead zone and forced vortex below impeller in DBD tank. Thus, the LES was employed here to estimate the magnitude of this vortex. In this case, the distributions of all velocity components in the same plane as above were calculated from:

$$U_{radial}(r) = \frac{\sum_{i=1}^{n}\frac{1}{2\pi}\int_0^{2\pi} U_{radial,i}(r,\theta)d\theta}{n} \quad (18)$$

$$U_{axial}(r) = \frac{\sum_{i=1}^{n}\frac{1}{2\pi}\int_0^{2\pi} U_{axial,i}(r,\theta)d\theta}{n} \quad (19)$$

$$U_{tangential}(r) = \frac{\sum_{i=1}^{n} \frac{1}{2\pi} \int_0^{2\pi} U_{tangential,i}(r,\theta) d\theta}{n} \quad (20)$$

and compared with the results obtained using standard k-ε model in Fig. 6.

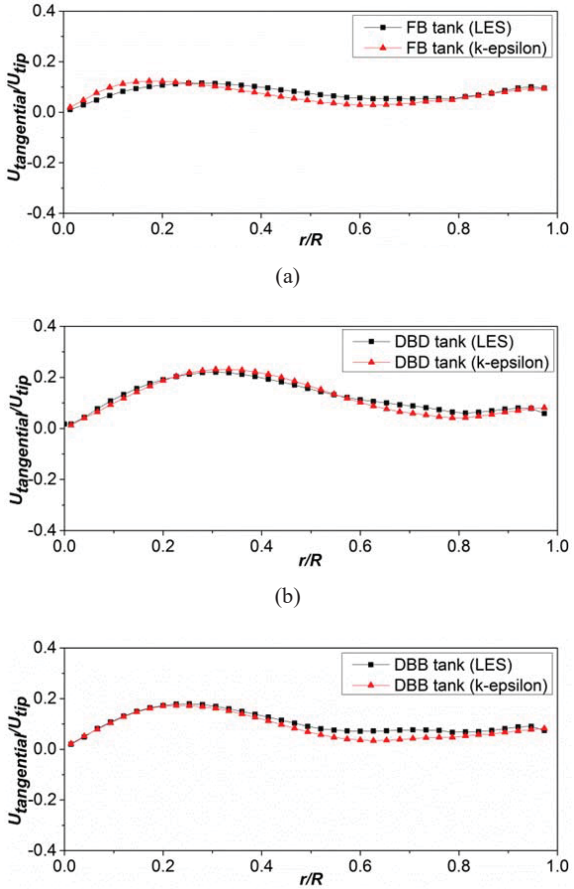

(a)

(b)

(c)

Fig. 6 Tangential velocity profiles predicted by standard k-ε model and LES: (a) FB tank; (b) DBD tank; (c) DBB tank

LES predicts slightly lower tangential velocities from centre to 0.25R and marginally higher tangential velocities from 0.3R to 0.7R in FB tank. It appears that the vortex predicted by the LES and standard k-ε model has similar trend, but its diameter predicted by k-ε model is smaller than that in FB tank. Figs. 6 (b) and (c) show that the liquid tangential velocity profiles predicted by both methods are similar in DBD and DBB tanks and minor differences can only be observed away from the vortex edge.

Generally, velocity profiles obtained by standard k-ε model showed similar trend and agree with well with LES results, which confirms the presence of dead zone area below the impeller in DBD tank. The bottom shape and baffles' length have significant effect on flow patterns and the efficiency of mixing in the region below the impeller.

C. Effect of Bottom Shape and Baffles' Length on Ionic Liquid Flow Field

Fig. 7 shows the time averaged vectors and the contours of velocity magnitude below the impeller when ionic liquid was mixed at an impeller speed of 440 rpm. The Reynolds number, *Re*, is 650, which indicates the flow is in transitional flow regime at this operation condition [1].

According to Fig. 7, the volume of dead zone below the impeller in DBD tank (Fig. 7 (b)) is significantly smaller than the one in fully turbulent mixing (Fig. 4 (b)). Fig. 7 also shows formation of the downward circulation loops, but the extent of radial-axial circulation is drastically reduced which is similar to the results reported by [24].

Secondary circulation flows were formed below the downward circulating loops in each stirred tank and the strongest were observed in flat bottom stirred tank (Fig. 7 (a)). The weak turbulence and secondary circulation loops have significant effect on mixing performance and it has been reported that additional recirculation zone and weak turbulent circulation flow will prolonged the mixing time [36], [37].

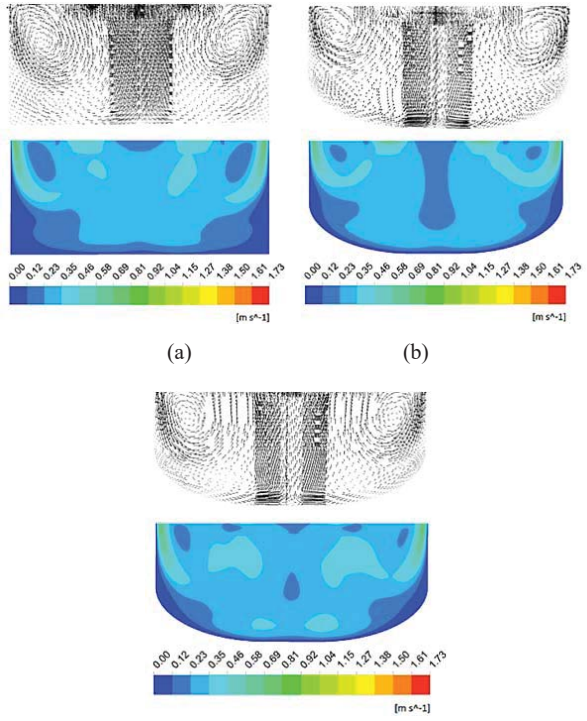

(a) (b)

(c)

Fig. 7 Velocity vectors and contours below the impeller in: (a) FB tank; (b) DBD tank; (c) DBB tank

The radial distribution of radial, axial and tangential velocities at the plane of 40 mm above the tank bottom in all three geometries are shown in Fig. 8. The data of velocity components were normalized by impeller tip velocity which is 1.73 m/s here. This plane is passing through the downward circulation loops, and radial velocity is negative between 0.3R and 0.9R. Neither the bottom shape nor baffles' length has

significant effect on radical velocity at this plane (Fig. 8 (a)). However axial velocity is slightly increased in dished bottom tanks (Fig. 8 (b)), which nearly have the same axial velocity at the plane centre. And axial velocity distributions in DBB tank are similar to that in FB tank away from this plane centre. The axial velocity in the baffles region (around 0.9*R*) was reduced when short baffles were employed in DBD tank which will hamper mixing intensity close to the tank wall. Fig. 8 (c) shows that the forced vortex formed below the impeller in each stirred tank. The change of bottom shape and extension of baffles do not cause marked change on the magnitude of vortex, which is very different from the one observed in turbulent flow (Fig. 5 (c)).

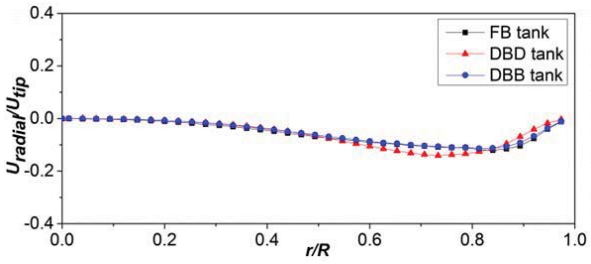

(a)

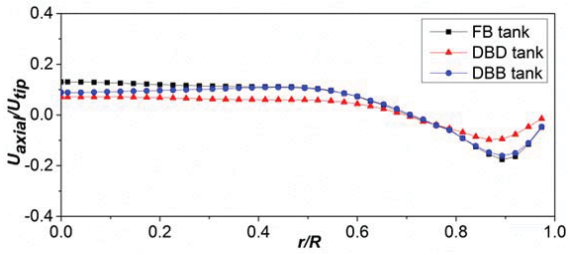

(b)

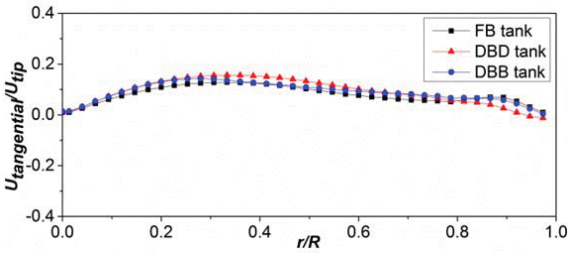

(c)

Fig. 8 Radial distributions of velocity components: (a) radial velocity, (b) axial velocity, (c) tangential velocity

D.Effect of Flow Regime on Flow Field

The velocities distributions in all investigated geometries in transitional flow (highly viscous ionic liquid) are compared with the velocities distributions in turbulent flow (water) from Figs. 9-11. The time-averaged data were sampled at the horizontal plane 40 mm above the tank bottom in all cases.

The radial velocity in turbulent flow is practically zero (Fig. 9 (a)) in flat bottom tank, as flow in this plane is almost axial/tangential. In the transitional flow (ionic liquid) the downward circulation was reduced and liquids started to flow towards impeller before they reached the tank bottom, therefore the radial velocity is negative away from this plane centre. The axial velocities just below the impeller and in the baffles region are substantially lower in transitional flow than in turbulent flow (Fig. 9 (b)). At this plane centre, axial velocity was reduced from $0.2U_{tip}$ to $0.13U_{tip}$ which implies that the intensity of mixing in ionic liquid system has substantially reduced [35].

The tangential velocity profiles in both types of flow are practically overlapping as shown Fig. 9 (c). The liquid viscosity did not cause significant effect on the tangential velocity component below the impeller at this plane.

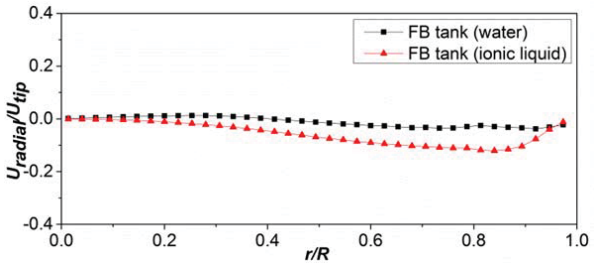

(a)

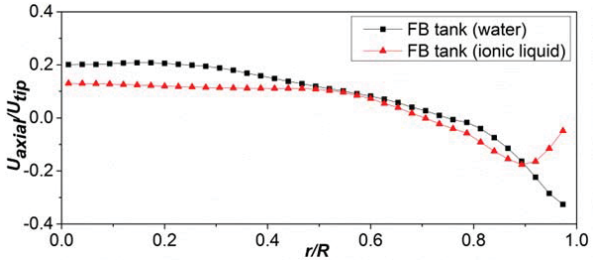

(b)

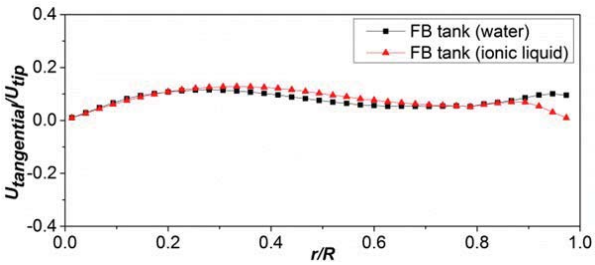

(c)

Fig. 9 Velocity components profiles of water and ionic liquid flow in FB tank: (a) radial velocity, (b) axial velocity, (c) tangential velocity

Fig. 10 compares velocity components of water turbulent flow and ionic liquid transitional flow in the DBD tank (baffles reaching dish level). As mentioned earlier, the bottom shape and baffles length did not have significant effect on the radial velocity profiles and the radial velocity components show similar trend in all tested tanks when liquid was operated in turbulent or transitional status. Therefore, Figs. 10 (a) and 11 (a) which compare the radial velocity components will not be

further discussed here. As can be observed in Fig. 10, there is however strong effect of flow regime on axial and tangential velocity profiles. In turbulent flow, the axial velocity at the centre of this plane is practically zero whilst at the same point the axial velocity of ionic liquid is approximately $0.07U_{tip}$ (Fig. 10 (b)). The same figure shows that the axial velocity in transitional flow is more uniform than in the turbulent flow and it only goes through weak minimum around the baffles. The strong reduction on peak value of tangential velocity in ionic liquid (Fig. 10 (c)) from $0.22U_{tip}$ to $0.15U_{tip}$ implies that the intensity of the forced vortex was greatly reduced in this region.

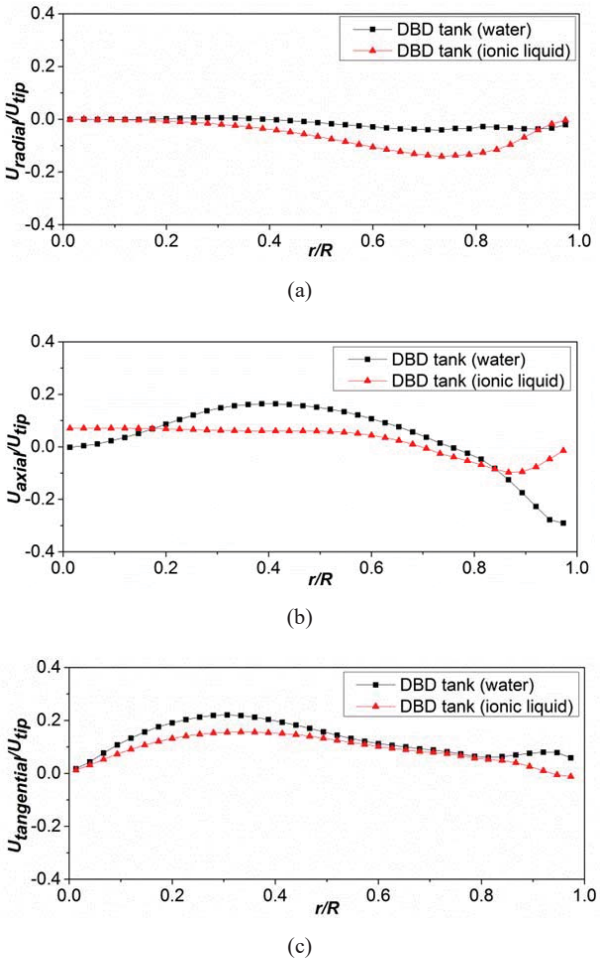

Fig. 10 Velocity components profiles of water and ionic liquid flow in DBD tank: (a) radial velocity; (b) axial velocity; (c) tangential velocity

Fig. 11 shows velocity components in turbulent flow and in transitional flow in DBB tank at a horizontal plane 40 mm above tank bottom. Similar to Fig. 9 (b), reduction of axial velocity at this plane was observed and the effect of baffles on promoting the flow in axial direction below the impeller is hindered when ionic liquid is agitated DBB tank. As can be seen in Figs. 11 (b) and (c), slightly decrease of axial and tangential velocities at this plane centre can be found when ionic liquid was used as operation liquid. While away from the plane centre, obvious reduction can be observed. Therefore, compared with water turbulent flow, the mixing in axial direction below the impeller is further diminished when ionic liquid is operated in DBB tank. Due to the high viscosity of ionic liquid, the peak tangential velocity below the impeller was reduced a lot (from $0.18U_{tip}$ to $0.14U_{tip}$) which implies that the magnitude of the forced vortex was reduced in this area.

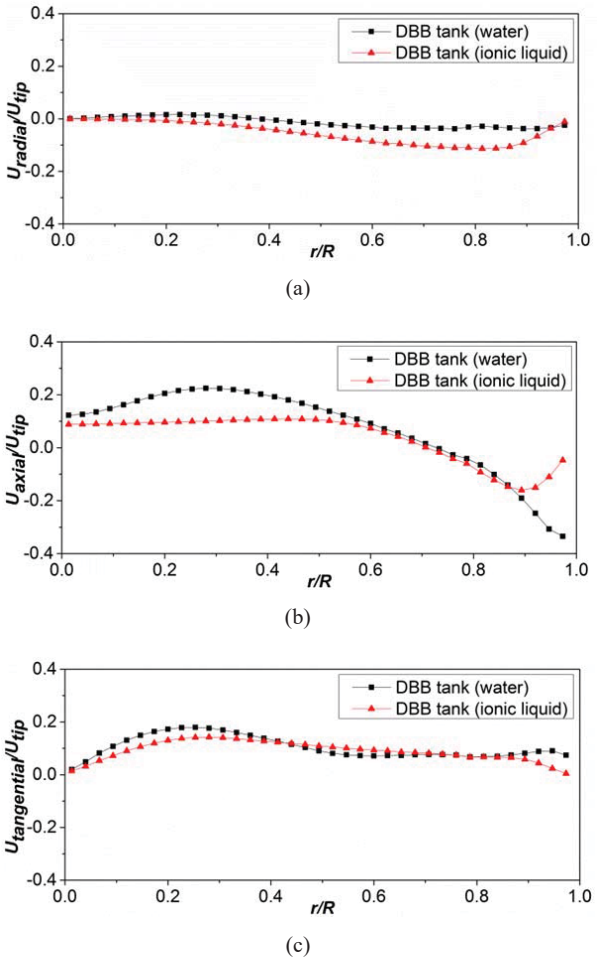

Fig. 11 Velocity components profiles of water and ionic liquid flow in DBB tank: (a) radial velocity, (b) axial velocity, (c) tangential velocity

Figs. 9-11 clearly show that flow regime, shape of the tank bottom and baffles length have significant effect on flow field in stirred tank. In transitional flow, liquid velocity close the tank wall is almost zero in all geometries, which indicates that liquid in this region is almost stagnant. The stagnant near wall region in stirred tank has significant effect on mixing performance of stirred tank, since it may cause concentration gradients near the wall and persist for a relative long time during mixing process hence prolonged the mixing time [38]. Unlike the characteristic water turbulent flow pattern agitated by Rushton turbine, the ionic liquid viscosity diminished the magnitude of the upward and downward circulation loops in all stirred tanks, and reducing the effect of baffles on generating flow in axial direction in FB tank and DBB tank. Maybe due to the effect of high liquid viscosity and secondary circulation

loops near the tank bottom, the short baffles have slightly effect on forming the dead zone area below the impeller disk in DBD tank in which large and obvious stagnant region can be observed in water turbulent flow. In water fully turbulent condition, the extension of baffles' length has significant effect on reducing the magnitude of the forced vortex below the impeller and increasing the flow velocity in axial direction, hence significantly enhancing the mixing efficiency in this area in dished bottom stirred tank. While this dead zone was reduced a lot when ionic liquid was used as operation liquid in DBD tank. Similar flow pattern and velocity components were identified in DBD and DBB tank below the impeller region. Thus, the disadvantage of DBD tank in mixing performance was reduced when liquid with high viscosity such as ionic liquid was used.

V. Conclusions

Turbulent flow fields in three stirred tanks with different geometries were simulated using standard *k-ε* model and LES. The ionic liquid transitional flow was modelled by LES. The results clearly show that the shapes of tank bottom, length of baffles and liquid viscosity have significant effect on flow pattern as well as the velocity profiles below the impeller. A strong vortex was formed below the impeller in DBD tank in water turbulent flow, which indicates that liquid below the impeller was not fully mixed. The axial flow was minimal below the impeller, thus mixing in this region was rather poor. This vortex formed a dead zone which might lead to an extensive coalescence in gas/liquid system and also to problems with suspending solid particles in liquid. The baffles extended to the bottom of the dished bottom tank reduced the magnitude of this vortex and increased axial velocity improving overall mixing performance. The velocity distributions predicted by LES were similar to the results obtained by standard *k-ε* model, which reinforces the conclusions based on these results.

The effect of baffles' length on the forced vortex volume below the impeller was greatly reduced in the ionic liquid transitional flow, especially in DBD tank. This may be attributed to the fact that the high viscosity of liquid reducing the extent of the downward and upward circulation loops and forming secondary circulation loops near the tank bottom. These secondary circulation loops may break the rotation below the impeller and promote the circulation flow near the tank bottom enhancing the mixing performance in DBD tank.

Overall, the flat bottom stirred tank due to its minimum magnitude of dead zone below the impeller when liquid was operated in fully turbulent flow, it has better mixing performance than DBD and DBB tank at the same operation condition. The DBD tank will form a large dead zone area below the impeller, which make it inefficient to mix the liquid below the impeller in turbulent flow. The DBB tank can greatly reduce the magnitude of this dead zone, which improves the mixing efficiency in dished bottom stirred tanks. Since dished bottom tanks are more widely used in mixing industry, similar tank geometries like DBB tank provides better mixing. The DBD and DBB tank have similar mixing performance below the impeller when flow was in transitional state, but DBB tank provides better axial mixing near baffles region. Therefore, DBB tank offers better mixing for viscous fluids such as ionic liquid.

References

[1] Paul, E.L., V.A. Atiemo-Obeng, and S.M. Kresta, *Handbook of industrial mixing science and practice*. 2004, John Wiley & Sons, Inc.: Canada.
[2] Smith, J.M., *Industrial needs for mixing research.* chemical Engineering Research and Design, 1990. 68.
[3] Bakker, A. and H.E.A. Van den Akker, *Single-phase flow in stirred reactors.* Chemical Engineering Research and Design, 1994. 72(A4): p. 583-593.
[4] Ng, K. and M. Yianneskis, *Observations on the distribution of energy dissipation in stirred vessels.* Chemical Engineering Research and Design, 2000. 78(3): p. 334-341.
[5] Kumaresan, T. and J.B. Joshi, *Effect of impeller design on the flow pattern and mixing in stirred tanks.* Chemical Engineering Journal, 2006. 115(3): p. 173-193.
[6] Bakker, A. and H.E.A. Van den Akker, *Gas-liquid contacting with axial flow impellers.* Chemical Engineering Research and Design, 1994. 72(A4): p. 573-582.
[7] Gimbun, J., C.D. Rielly, and Z.K. Nagy, *Modelling of mass transfer in gas–liquid stirred tanks agitated by Rushton turbine and CD-6 impeller: A scale-up study.* Chemical Engineering Research and Design, 2009. 87(4): p. 437-451.
[8] Joshi, J.B., et al., *CFD Simulation of stirred tanks: comparison of turbulence models. part i: radial flow impellers.* Canadian Journal of Chemical Engineering, 2011. 89(1): p. 23-82.
[9] Joshi, J.B., et al., *CFD simulation of stirred tanks: comparison of turbulence models (part ii: axial flow impellers, multiple impellers and multiphase dispersions).* Canadian Journal of Chemical Engineering, 2011. 89(4): p. 754-816.
[10] Bakker, A. and L.M. Oshinowo, *Modelling of turbulence in stirred vessels using large eddy simulation.* Chemical Engineering Research and Design, 2004. 82(9): p. 1169-1178.
[11] Derksen, J. and H.E.A. Van den Akker, *Large eddy simulations on the flow driven by a Rushton turbine.* AIChE Journal, 1999. 45(2): p. 209-221.
[12] Eggels, J.G.M., *Direct and large-eddy simulation of turbulent fluid flow using the Lattice-Boltzmann scheme.* International Journal of Heat and Fluid Flow, 1996. 17(3): p. 307-323.
[13] Deglon, D.A. and C.J. Meyer, *CFD modelling of stirred tanks: Numerical considerations.* Minerals Engineering, 2006. 19(10): p. 1059-1068.
[14] Aubin, J., D.F. Fletcher, and C. Xuereb, *Modeling turbulent flow in stirred tanks with CFD: The influence of the modeling approach, turbulence model and numerical scheme.* Experimental Thermal and Fluid Science, 2004. 28(5): p. 431-445.
[15] Wu, H. and G.K. Patterson, *Laser-Doppler measurements of turbulent-flow parameters in a stirred mixer.* Chemical Engineering Science, 1989. 44(10): p. 2207-2221.
[16] Roy, S., S. Acharya, and M.D. Cloeter, *Flow structure and the effect of macro-instabilities in a pitched-blade stirred tank.* Chemical Engineering Science, 2010. 65(10): p. 3009-3024.
[17] Deen, N.G., T. Solberg, and B.H. Hjertager, *Flow generated by an aerated rushton impeller: two-phase piv experiments and numerical simulations.* The Canadian Journal of Chemical Engineering, 2002. 80(4): p. 1-15.
[18] Gabriele, A., A.W. Nienow, and M.J.H. Simmons, *Use of angle resolved PIV to estimate local specific energy dissipation rates for up- and down-pumping pitched blade agitators in a stirred tank.* Chemical Engineering Science, 2009. 64(1): p. 126-143.
[19] Jaworski, Z. and B. Zakrzewska, *Modelling of the turbulent wall jet generated by a pitched blade turbine impeller: the effect of turbulence model.* Chemical Engineering Research and Design, 2002. 80(8): p. 846-854.
[20] Ochieng, A. and M.S. Onyango, *CFD simulation of solids suspension in stirred tanks: review.* Hemijska Industrija, 2010. 64(5): p. 365-374.
[21] Lu, W.-M., H.-Z. Wu, and M.-Y. Ju, *Effects of baffle design on the liquid mixing in an aerated stirred tank with standard Rushton turbine impellers.* Chemical Engineering Science, 1997. 52(21–22): p. 3843-3851.

[22] Karcz, J. and M. Major, *An effect of a baffle length on the power consumption in an agitated vessel*. Chemical Engineering and Processing: Process Intensification, 1998. 37(3): p. 249-256.
[23] Haque, J.N., et al., *Free-surface turbulent flow induced by a Rushton turbine in an unbaffled dish-bottom stirred tank reactor: LDV measurements and CFD simulations.* The Canadian Journal of Chemical Engineering, 2011. 89(4): p. 745-753.
[24] Jaworski, Z., et al., *Sliding mesh simulation of transitional, non-newtonian flow in a baffled stirred tank*, in *Computation of Three-Dimensional Complex Flows*, M. Deville, S. Gavrilakis, and I. Ryhming, Editors. 1996, Vieweg+Teubner Verlag. p. 109-115.
[25] Yang, F., et al., *Mixing of initially stratified miscible fluids in an eccentric stirred tank: Detached eddy simulation and volume of fluid study*. Korean Journal of Chemical Engineering, 2013. 30(10): p. 1843-1854.
[26] Woziwodzki, S., L. Broniarz-Press, and M. Ochowiak, *Effect of eccentricity on transitional mixing in vessel equipped with turbine impellers.* Chemical Engineering Research and Design, 2010. 88(12): p. 1607-1614.
[27] Versteeg, H.K. and W. Malalasekera, *An introduction to computational fluid dynamics the finite volume method*. 2007, Pearson Education Ltd.
[28] ANSYS, *ANSYS FLUENT theory guide. Pennsylvania: ANSYS Ltd*. 2011.
[29] Hartmann, H., et al., *Assessment of large eddy and RANS stirred tank simulations by means of LDA.* Chemical Engineering Science, 2004. 59(12): p. 2419-2432.
[30] Fan, J., Y. Wang, and W. Fei, *Large eddy simulations of flow instabilities in a stirred tank generated by a Rushton turbine.* Chinese Journal of Chemical Engineering, 2007. 15(2): p. 200-208.
[31] Zadghaffari, R., J.S. Moghaddas, and J. Revstedt, *Large-eddy simulation of turbulent flow in a stirred tank driven by a Rushton turbine.* Computers & Fluids, 2010. 39(7): p. 1183-1190.
[32] Delafosse, A., et al., *LES and URANS simulations of hydrodynamics in mixing tank: Comparison to PIV experiments.* Chemical Engineering Research and Design, 2008. 86(12): p. 1322-1330.
[33] SHAW, C.T., *Using computational fluid dynamics*. 1992, New York: Prentice Hall.
[34] Busciglio, A., G. Caputo, and F. Scargiali, *Free-surface shape in unbaffled stirred vessels: Experimental study via digital image analysis.* Chemical Engineering Science, 2013. 104(0): p. 868-880.
[35] Lamarque, N., et al., *Large-eddy simulation of the turbulent free-surface flow in an unbaffled stirred tank reactor.* Chemical Engineering Science, 2010. 65(15): p. 4307-4322.
[36] Murthy Shekhar, S. and S. Jayanti, *CFD study of power and mixing time for paddle mixing in unbaffled vessels.* Chemical Engineering Research and Design, 2002. 80(5): p. 482-498.
[37] Sano, Y. and H. Usui, *Interrelations among mixing time, power number and discharge flow rate number in baffled mixing vessels.* Journal of Chemical Engineering of Japan, 1985. 18(1): p. 47-52.
[38] Lamberto, D.J., M.M. Alvarez, and F.J. Muzzio, *Experimental and computational investigation of the laminar flow structure in a stirred tank.* Chemical Engineering Science, 1999. 54(7): p. 919-942.